Fibre Orientation Probability Maps from *Q*-Ball and the Model-Based Bootstrap – A Potential Segmentation Tool

H. A. Haroon[1], K. V. Embleton[1,2], and G. J. Parker[1]

[1]Imaging Science & Biomedical Engineering, The University of Manchester, Manchester, England, United Kingdom, [2]School of Psychological Sciences, The University of Manchester, Manchester, England, United Kingdom

Introduction We have previously shown the comparability of the output of model-based residual (MBR) bootstrapping with the output from conventional bootstrapping when applied to the *q*-ball[1] analysis of DWI datasets[2]. Model-based residual bootstrap enables quantification of the uncertainty in the inferred fibre orientation for probabilistic fibre tracking using a single HARDI dataset[3,4,5]. Here we present probability maps of observing *n* fibre orientations estimated by MBR bootstrapping over *i* iterations on a voxel-by-voxel basis. These probability maps provide information for the classification of tissues based on their microstructural orientation complexity.

Methods HARDI data were acquired with two different protocols in two healthy subjects on a 3T Philips Achieva scanner (Philips Medical Systems, Best, Netherlands) using an 8-element SENSE head coil. *Dataset 1:* PGSE EPI with TE = 54ms, TR = 6000ms, G_{max} = 62mT/m, partial Fourier factor 0.679, 112 × 112 matrix reconstructed to 128 x 128, reconstructed resolution 1.84 mm, slice thickness 2.1 mm, 34 slices, 61 diffusion sensitisation directions at b = 1200s/mm^2 (Δ = 28.37ms, δ = 13.52ms), 1 at b = 0, SENSE factor = 2.5, total imaging time 7 min. This sequence was repeated 8 times in the same volunteer to provide a conventional bootstrapping dataset. All diffusion-sensitised images were registered to the corresponding b = 0 image within each slice location and for all scanning repetitions to the first scan, using a 2D affine registration[6]. *Dataset 2:* PGSE EPI with the same parameters as in Dataset 1 apart from TE = 59 ms, TR = 13,091 ms, cardiac gating, reconstructed resolution 1.875 mm, 60 contiguous slices, b = 1200s/mm^2 (Δ = 29.8ms, δ = 13.1ms). Phase encoding was performed in right-left and left-right directions for each diffusion gradient orientation and slice to allow correction for susceptibility and eddy current-induced distortion[7]. The total imaging time = 2 × 16 minutes.

Conventional Bootstrapping: Conventional bootstrapping was applied to the 8 repetitions of Dataset 1. For each of 1000 iterations, a new image set was created by randomly taking a voxel from any of the 8 repetitions, in the same slice and in matching diffusion-sensitising directions, on a voxel-by-voxel basis, in a single mid-brain slice. The image set created by each bootstrap sampling was then processed using the *q*-ball method, which generates orientation distribution functions (ODF)[1], the peaks of which relate to the principle underlying fibre orientations (one or more)[8]. The ODF values are reconstructed at 642 discrete points on a unit sphere given by a three-fold tessellated icosahedron. *MBR Bootstrapping:* A given dataset was first processed with *q*-ball to generate ODFs. Using the number of fibres extracted in each voxel from the ODFs we fitted one, two or three diffusion tensors to the original diffusion-weighted signal acquired[9], or assumed isotropic diffusion if the number of fibres extracted using *q*-ball was greater than three. The predicted signal was then recovered using the fitted diffusion tensors[9]. Residuals were calculated by taking the difference between the predicted diffusion-weighted signal from the multi-tensor fitting and the original diffusion-weighted signal. A new image set was created by randomly shuffling the residuals, for any given voxel, amongst all the diffusion-encoding directions and then adding them on to the predicted diffusion-weighted signals. The image set created by each bootstrap sampling was processed with *q*-ball to extract the estimates of underlying fibre orientations, as described above using 1000 iterations in a single slice for Dataset 1 and over 100 iterations in a whole-brain volume for Dataset 2.

Probability Maps of Fibre Orientation: The probability of observing *n* fiber orientations was determined from the frequency of finding *n* fiber orientations over *i* bootstrap iterations, with both the MBR and conventional bootstrap methods in Dataset 1 (i = 1000) and with the MBR bootstrap method in Dataset 2 (i = 100). We chose n = 1, 2, 3 and greater than 3.

Results Fig. 1(a) shows a generalised fractional anisotropy (GFA) map of the single slice in Dataset 1 used to create the maps in Fig. 1(b) of the probability of observing *n* fiber orientations over 1000 bootstrap iterations, with conventional bootstrapping (Fig. 1(b) left column) and MBR bootstrapping (Fig. 1(b) right column). Good concordance is observed between the two bootstrap methods. The highest probability of observing n = 1 (Fig. 1(b) 1st row) is, as expected, concentrated in the core of the white matter tracts, although relatively high probabilities are also observed within the thalamus (red arrow). High probabilities of n = 2 (Fig. 1(b) 2nd row) are more widespread beyond the core of tracts than is the case for n = 1 populations, although the probabilities for n = 2 are generally lower. There is around a 50% chance of two fiber populations being observed in some areas within the thalamus (red arrow) and in a number of deep grey matter areas. The MBR bootstrap generally estimates a slightly higher probability of two fiber populations than the conventional method. There is a more mixed picture in estimating n = 3 (Fig. 1(b) 3rd row), although both methods indicate that the probability of observing this configuration is low in most regions in this slice. Interestingly there is an increased probability of observing three distinct orientations in the thalamus (red arrow), with the conventional bootstrap method also indicating relatively high probabilities at the border between the cortex and white matter, and within the cortex itself. The probability of observing n > 3 (Fig. 1(b) 4th row) is high in most cortical regions and in the putamen (green arrow) and head of the caudate nucleus (turquoise arrow). We assume that these are indicative of noise and represent near-isotropic diffusion, as indicated in the GFA map in Fig. 1(a). Fig. 2 shows orthogonal views of the volume maps for GFA (Fig. 2 1st column), n = 1 (Fig. 2 2nd column), n = 2 (Fig. 2 3rd column), n = 3 (Fig. 2 4th column) and n > 3 (Fig. 2 5th column) in Dataset 2 over 100 bootstrap iterations with MBR bootstrapping. The green crosshairs in Fig. 2 are centred on an area of white matter (Fig. 2 1st column) known to contain crossing fibres, which is identified as having a very high probability for n = 2 (Fig. 2 3rd column) but negligible probability on all the other maps.

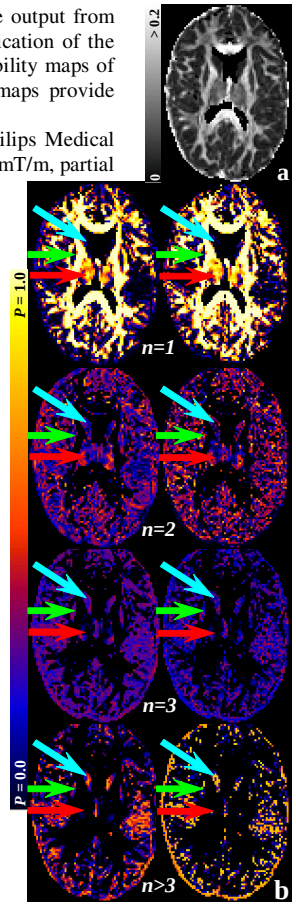

Figure 1

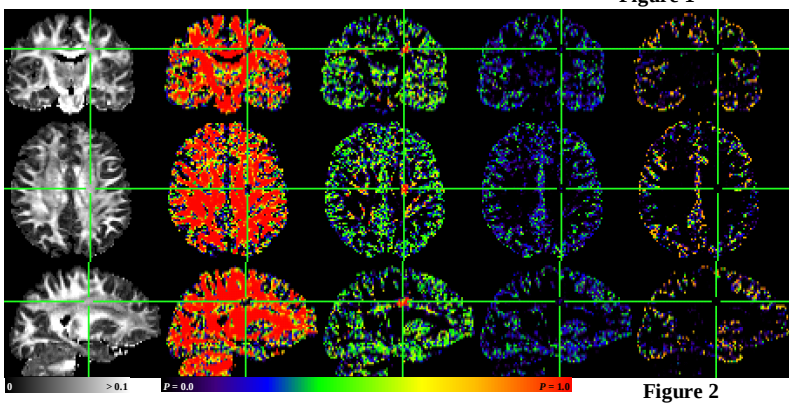

Figure 2

Conclusion Both conventional and model-based residual bootstrapping provide a means by which the microstructural complexity of tissue, as reflected in the HARDI diffusion signal, may be estimated. The probability of finding any given configuration reflects the underlying tissue microscopic complexity, macroscopic partial volume, and data noise levels. This information will be of use in probabilistic tractography and in monitoring changes in tissue complexity due to disease or developmental processes.

References 1. Tuch, DS, *Magn Reson Med*, **52**: 1358, 2004. 2. Haroon, HA & Parker, GJ, *Proc ISMRM*, 903, 2007. 3. Whitcher, B, *et al*, *Proc ISMRM*, 1333, 2005. 4. Jones, DK, *Proc ISMRM*, 435, 2006. 5. Berman, JI, *et al*, *Proc ISMRM*, 1471, 2007. 6. Smith, SM, *et al*, *NeuroImage*, **23**(S1): 208, 2004. 7. Embleton, KV, *et al*, *Proc ISMRM*, 1070, 2006. 8. Fonteijn, HMJ, *et al*, *IEEE Trans Med Imaging*, **26**: 1515, 2007. 9. Alexander, DC, *et al*, *Magn Reson Med*, **48**: 331, 2002.

Acknowledgements This work is supported by the BBSRC (grant # BB/E002226/1) and the MRC (grant # G0501632). We'd like to thank Dr David Tuch (Novartis) for providing his original *q*-ball code.